CHAPTER 3

METHODOLOGY

General methodology for simulation of physiology modeling is introduced first in this chapter to explain how to relate system modeling, such as parametric model, model validation, governing equation, boundary condition setting and equation solving, to physiological system. Two methodologies for stresses and strains distributions of murine aortic vessel in three-dimension three-layer abdominal aortic wall based on *in vivo* ultrasound imaging and stresses and strains distributions of human aortic vessel in three-dimension five-layer aortic wall based on *in vivo* ultrasound imaging are then expressed.

We had firstly applied mechanical modeling of blood vessel to murine aortic vessel experimental data. The new mechanical modeling of aortic vessel can determine stress and strain distributions in all principal three directions of longitudinal, circumferential and radial directions and in multilayer. More realistic properties of aortic which well known to be as anisotropic and nonlinear material are also included in this study. Fiber-reinforced constitutive equation is suitable employed for all three major layers of aortic wall separated by considering histology of each aortic layer. Advantages of *in vivo* noninvasive ultrasound imaging provide important data of aortic wall movement along cardiac cycle time. Stress and strain distributions can be illustrated and interpreted. This advantage of combination of three-dimension three-layer fiber-reinforced aortic vessel modeling for stress and strain predictions and in vivo noninvasive experimental data has been first proposed on this study.

Consequently, the new mechanical modeling has been extend to use with more realistic aortic vessel by involve with more number of aortic layers and more constitutive equations and to then use as implement to predict and illustrate rupturing of the aortic vessel which has also been firstly introduced on this study. The new developed model is applied to determine stresses and strains distributions of human aortic vessel in three-dimension five-layer aortic wall based on *in vivo* ultrasound imaging. Two constitutive equations are suitable employed for all five layers of aortic wall separated by considering histology of each aortic layer. Stress and strain distributions can be illustrated and interpreted. Mapping of rupture area and rupture risk of aortic wall subjected by various luminal pressures can be performed by using critical stress and strain criterion.

To derive equations involving with the modeling from governing equation, authors would reasonably like to use notation for equations in from of tensor to allow reader easier understand global system of the modeling and can follow complexity of equations system. There are a number of basics tensor operations that may be conduct tensors and again produce a tensor. These tensor operations are not expressed on this chapter. One of several ways to find out these tensor operations is by using advanced mathematics books.

Methodology for simulation of physiology modeling to construct constitutive equation for three dimensional stress and strain relationship model and predict stress and strain distribution in aortic vessel wall is show as schematic chart in Figure 3.1 and could be explained as following.

3.1. Simulation of physiology modeling

Simulation of physiology modeling is the process of solving the model (the equations that are the realization of the model) to examine its output behavior. This process typically involves examining one or more of the parameters thus performing computer is needed to experiment on the model. During model building, simulation could be performed to clarify aspects of system behavior to determine whether a proposed model representation is appropriate. This is done by comparison of the model output with experimental data from the same situation. When carried out on a complete, validation model, simulation yields output responses that provide information on system behavior. Depending on the modeling purpose, this information assists in describing the system, predicting behavior, or yielding additional insights.

Complete mathematical model is firstly needed. All its parameters are specified and initial conditions are defined for all the variables. If the model is not complete, there has unspecified parameter values, parameter estimation technique must be employed. Once a complete model is available, it is implemented on the computer. If model equations cannot be solved analytically, a numerical solution of the system is needed.

Methodology for physiology modeling construction consists of 2 parts, is shown in Figure 3.1, which are collecting physiological data of physiological system of aortic vessel (physiological experiment) and modeling the system (data analysis).

Collecting physiological data of physiological system Physiological experiment data can represent physiological behavior. Experimental data from *in vivo*-noninvasive aortic vessel imaging technique using experimental data in animal

such as rat are used. The qualitative data, the imaging data, then must be conversed to be quantitative data, displacement data. This quantitative data are used to consider in the system modeling.

Modeling the system Model of the system is physiologically based by mathematically explanation that can describe directly to physiology of aortic vessel. Hence, a prior knowledge and reasonable assumptions are required.

3.1.1. Modeling the system (data analysis)

To perform physiological data for modeling the system, both a model structure and fully determined parameters corresponding to that structure are required. In the other word, a complete model is required. However, such a model has not yet established. Therefore, at least one candidate model is selected. A model is incomplete; it will be due to some unknown parameter value.

The solution from this problem requires data. The input and output data from experiment must contain that part of model with the unknown parameter values. In the process, data are mapped into parameter values by the model, where error can occur in both the data and model. Modeling the system is also called mechanical modeling.

3.1.2. Parametric model

The experimental data must be rich enough to estimate all the unknown parameters. Problem is a mismatch between the complexity of the model and the richness of the data which mean that model is too complex or too many unknown parameters for available data or the data are not sufficient for the model provided.

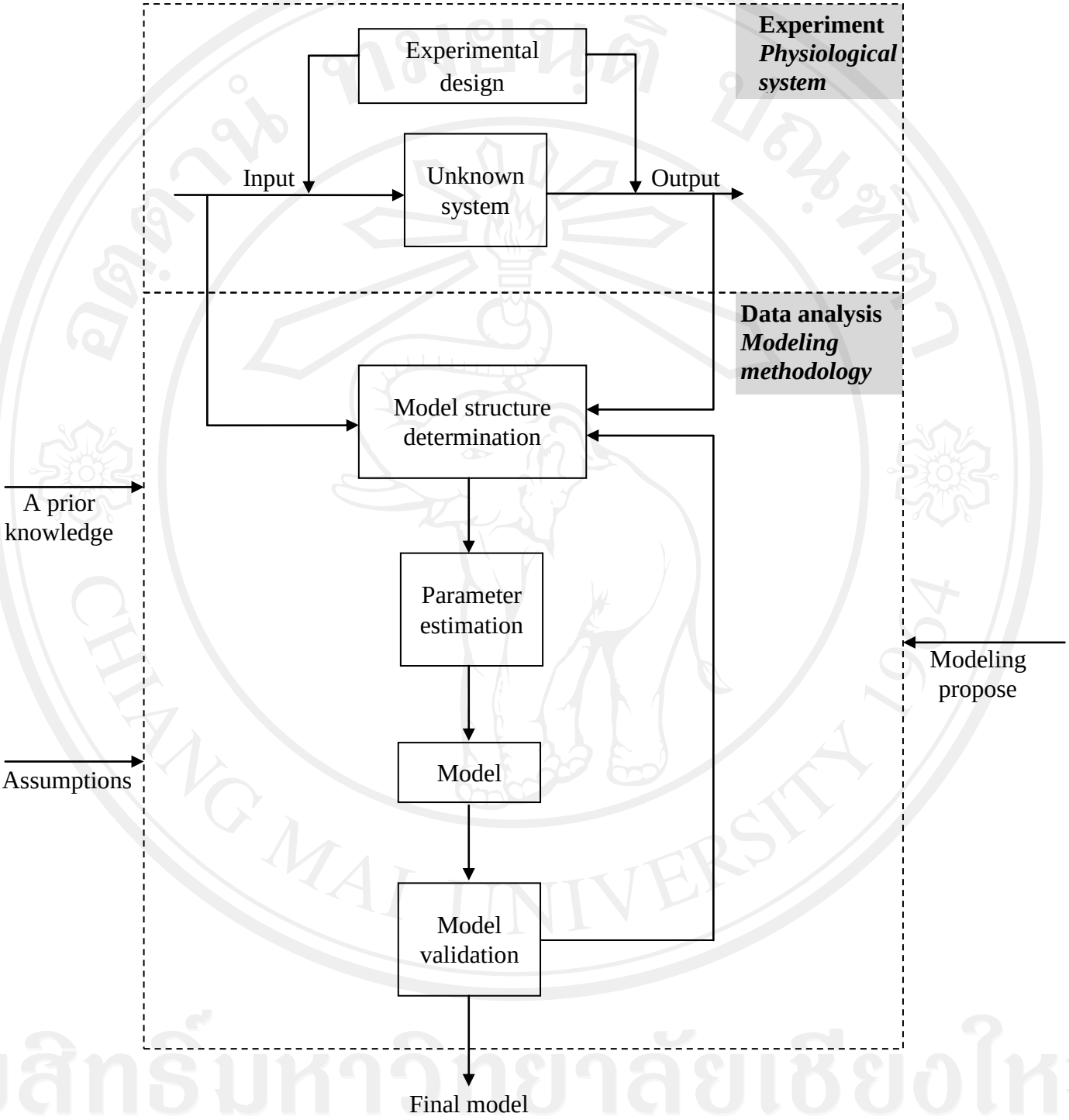

Figure 3.1 Methodology for simulation of physiology modeling

Existed techniques for parameter estimation are most widely adopted such as linear or nonlinear least squares. These require for a prior knowledge or assumptions regarding the statistics of the situation being model.

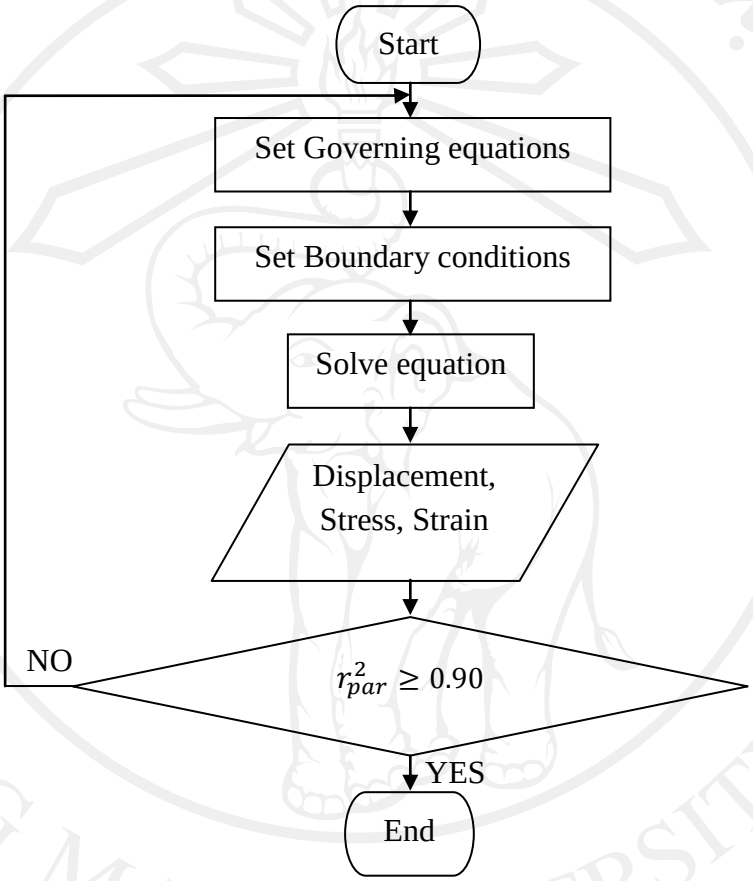

Figure 3.2 Modeling the system

3.1.3. Model validation

Validating a model is essentially whether the model is good enough in relation to its intended purpose. A valid model is one that has successfully passed through the validation process. Validation is integral to the overall modeling process. At the stage of validity testing during the process of model formulation, the model is assumed that the model is complete. That is, it has no unspecified parameters. The

essence of the validation process at this stage is shown in Figure 3.1 and Figure 3.2. The process is dependent upon model propose. That might be testing the appropriateness of model structure in relation to any intended use for hypothesis testing parameters that would be meaningful in the context of specific disease. Changing in parameter values could correspond to the change from a healthy state to a diseased state. Dependent upon propose, features of the model and system data must corresponded sufficiently for the same input, there have an acceptably small difference between them. In the other word, within the necessary domain of validity, there is testing whether the model is credible. The validation process is to compare the model and physiological behavior by estimate relevant parameters by minimizes function of mean square error of pressures. Any mismatch between them should be analyzed for plausibility of behavior. Additional explanation of modeling the system or mechanical modeling in the parts of governing equation setting, boundary conditions setting and equation solving showing in Figure 3.3 can be described.

3.1.4. Governing equation

Setting Knowledge of continuum mechanics is required to construct mechanical modeling using elasticity and deformation theory. Mechanical modeling is shown in Figure 3.3. Governing equation consist of five equations which are conservation equation of mass, conservation equation of momentum, conservation equation of energy, deformation equation and constitutive equation.

Deformation equation usually well known as strain and displacement relationship including Lagrangian coordinate, Spatial coordinate, Deformation

gradient, Green's deformation tensor, Cauchy deformation tensor, Lagrangian finite strain tensor, Eulerian finite strain tensor.

Geometry and coordination are considered to appropriate with anatomy of aortic vessel. The geometry of aortic vessel might be considered as symmetry or asymmetry in longitudinal axis and coordination might be considered either Cartesian coordination (X,Y,Z) or cylindrical coordination (R, Θ,Z).

Strain and displacement relationship equation is also called motion equation. Motion equation is the mapping equation which describes motion and deformation of aortic vessel that is assumed to satisfy the following conditions; the function is continuously differentiable, the function is one-to-one and the jacobian determinant satisfies (J=det $\boldsymbol{F}$) the condition J>0.

Constitutive equation is equation which describes aortic vessel behavior and relates stress to correspond with deformation. The formulation of constitutive equation consist of five steps which are delineation of general characteristics of interest, establishing an appropriate theoretical framework quantification, identification of specific functional forms of the constitutive equation, calculation of the value of the associated material parameters, evaluation of the predictive capability of the final relation. Assumptions of properties of aortic vessel regard to anatomy and physiology, might be selected from these; homogeneous/ heterogeneous/ composite material, compressible/ incompressible material, isotropic/ anisotropic material, hyperelastic/ pseudoelastic/ ramdomly elastic/ poroelastic/ viscoelastic material.

Stress and strain relationship can be written in form of equation which is importance to represent aortic vessel behavior. Differentiation of strain energy

density function respect to strain with lowest potential energy method is obtained stress function. Constitutive equation could be obtained.

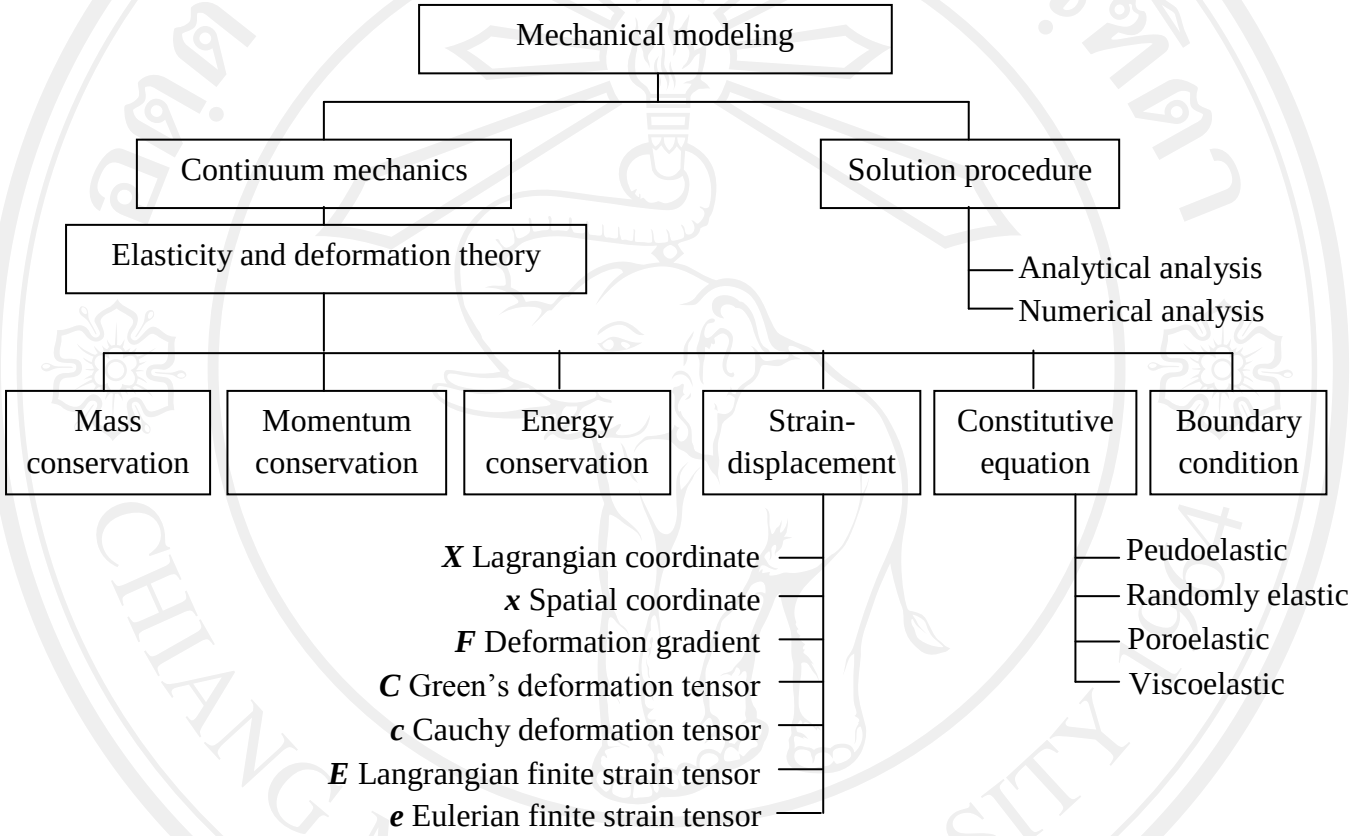

Figure 3.3 Mechanical Modeling

3.1.5. Boundary condition setting

Boundary condition is pressure load from blood flow inside aortic vessel subjected to inside wall of aortic vessel and depend on physiology to obtain specific equations.

3.1.6. Equation solving

This stage is to solve the problem by selecting the suitable method. An analytical solution is one of method. In some case, analytical solution requires the solution of ordinary or partial differential equations which are not usually obtainable because of the complication geometry, loading, and material properties. Hence, numerical methods could be reliability, such as finite element method, for acceptable solutions.

Conclusions of the research will be obtained which are constitutive equation for three dimensional stress and strain relationship model of aortic vessel and prediction of stress and strain distribution across aortic vessel.

3.2. Mechanical modeling of blood vessel for murine aortic vessel

Vascular system has the aorta which acts as both conduit and an elastic chamber. The elastic of aorta serves to convert pulsatile flow pumped by heart to steady flow in peripheral vessels. Atherosclerosis, the common disease of arterial wall, is a disease usually located within large arteries (Yang and Vafai, 2006) and buildup of atherosclerosis plaque usually associates with pathological changes of intimal component of vascular layers (Holzapfel and Gasser, 2001; Holzapfel, 2001). One of the implications of the structural changes is the change in mechanical properties of the blood vessel. Stress and strain are used to represent the mechanical properties. As mention, it could be observed that disease location associates with position on artery tree and inside wall. So, stress and strain distribution in multidimensional and multilayers should be predicted. In order to friendly for patient, advantage of imaging technology should be used as additional data, especially the

ultrasound scanning. Ultrasound scanning is non-invasive medical test that has no needles or injections and is usually painless. Hence, this section proposes to predict stresses and strains distributions in coordinate of three dimensions and in three major layers of abdominal aortic wall based on *in vivo* ultrasound imaging.

3.2.1. Experimental data harvest

3.2.1.1. Luminal pressure

Luminal pressure acted to the inside wall causes vascular wall movement. Wild-type C57BL/6 male mouse is obtained from the Jackson (Bar Harbor, ME) and Taconic (German town, NY) Laboratories. All procedures are approved by the Institutional Animal Care and use committee of Columbia University. Abdominal aorta of mouse is canulated using an ultraminiature pressure catheter through the mouse carotid artery and introduces into the abdominal aortic region to provide both of luminal pressure and ECG signals (see Figure 3.4- Figure 3.6).

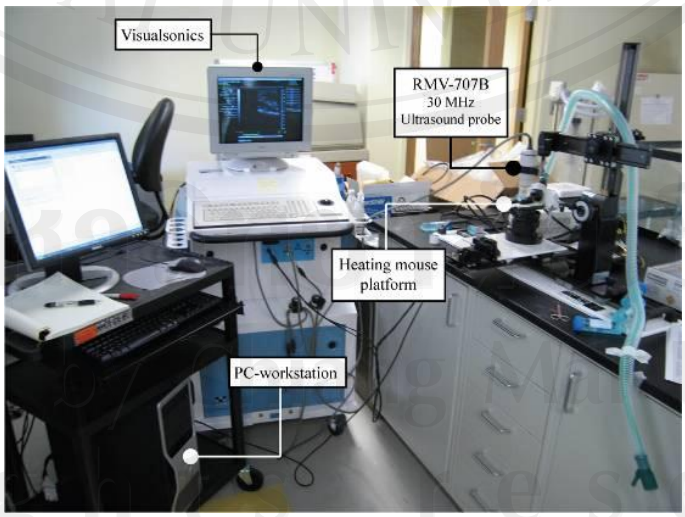

Figure 3.4 The system set up of mouse experiments (Danpinid, 2010)

A. 30 MHz ultrasound probe

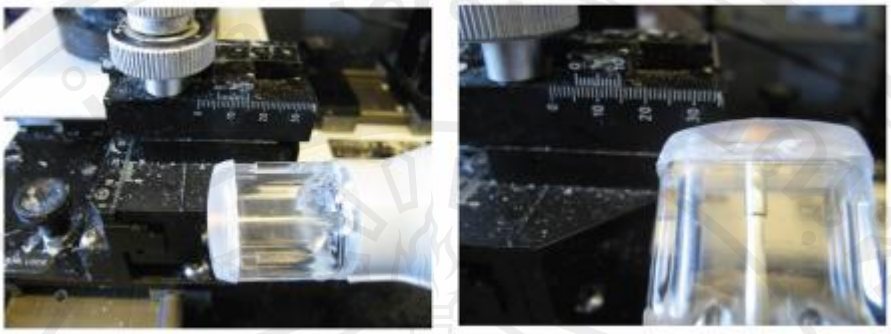

B. Mouse platform

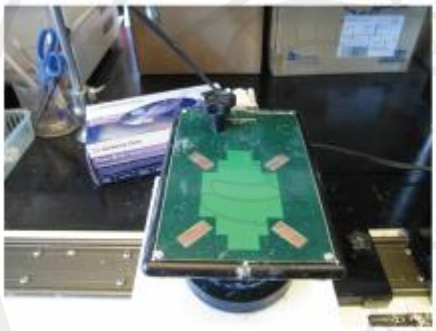

Heart rate and temperature recorder

C. Experimental assembly

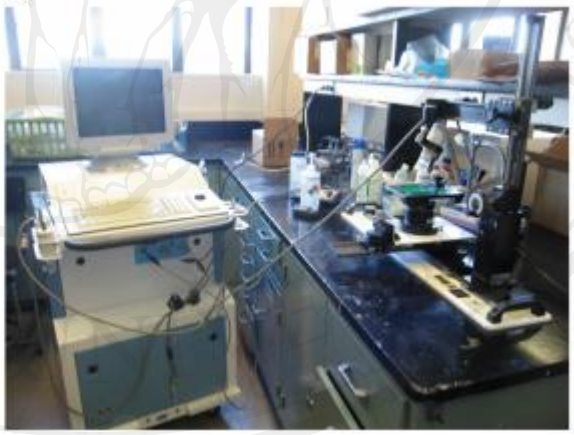

Figure 3.5 A. 30 MHz ultrasound probe B. Mouse platform (left) and heart rate and temperature recorder (right) C. Experimental assembly with Vevo 770 (VisualSonics), 30 MHz ultrasound probe, mouse platform (Danpinid, 2010)

3.2.1.2. Displacement

Five wild-type C57BL/6 male mice (7-10 month old) are obtained from the Jackson (Bar Harbor, ME) and Taconic (German town, NY) Laboratories. All procedures are approved by the Institutional Animal Care and use committee of Columbia University. The inside and outside aortic diameters of abdominal aortic wall are clearly obtained through manual tracing on the B-mode image of ultrasound imaging with higher frame rate of 8 MHz. Then, the radial incremental displacements of the inside and outside walls are determined which then accumulate to obtain the wall diameter variation over a cardiac cycle. The luminal pressure and aortic wall diameter variations are matched using the corresponding ECG by align the maximum and minimum peaks of the luminal pressure and diameter variations. All experimental data based on ultrasound then are used as importance inputs in mechanical model (see more details in Danpinid (2010), Danpinid *et al.* (2010) and Fujikura *et al.* (2007)). (Experimental data had supported from Ultrasound and Elasticity Imaging Laboratory (UEIL), Biomedical Engineering and Radiology, Columbia University, New York, USA).

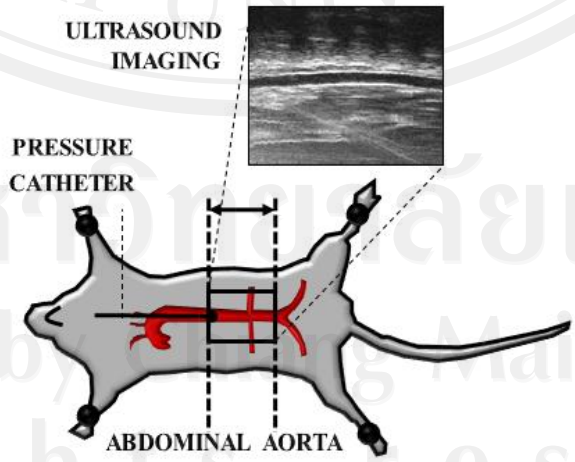

Figure 3.6 Experimental methodology with healthy mouse in abdomen

3.2.2. Mechanical modeling

3.2.2.1. Continuum mechanics

The mathematical description of deformation, the body occupy in the reference configuration Ω_o. When the body is deformed, every particle at point $\boldsymbol{X}(R, \Theta, Z)$ transforms to new position at point $\boldsymbol{x}(r, \theta, z)$ in deformed configuration Ω. Configurations of artery are shown in Figure 2.8. R, Θ and Z are radial, angular (circumferential) and longitudinal positions in reference configuration and r, θ and z are radial, angular (circumferential) and longitudinal positions in deformed (current) configuration The transformation gradient could be determined by following equation.

$$\boldsymbol{F} = \frac{\partial \boldsymbol{x}}{\partial \boldsymbol{X}} \tag{3.1}$$

Right and left Cauchy Green tensor associate with $\boldsymbol{F}$ as following.

$$\boldsymbol{C} = \boldsymbol{F}^T\boldsymbol{F}\ ,\ \boldsymbol{b} = \boldsymbol{F}\boldsymbol{F}^T \tag{3.2}$$

So, the Green-Lagrange strain tensor could be introduced as Equation (3.3).

$$\boldsymbol{E} = \frac{1}{2}(\boldsymbol{C} - \boldsymbol{I}) \tag{3.3}$$

where $\boldsymbol{I}$ denotes the second order unit tensor.

For stress response of the artery, Cauchy stress tensor $\boldsymbol{\sigma}$ relates to Green-Lagrange strain tensor $\boldsymbol{E}$ via transformation ($\boldsymbol{\sigma} = J^{-1}\boldsymbol{F}\boldsymbol{S}\boldsymbol{F}^{T}$) the Piola Kirchhoff stress tensor $\boldsymbol{S}$ which is the first derivative $\left(\frac{\partial \Psi}{\partial \boldsymbol{E}}\right)$ of strain energy function Ψ respected to Green-Lagrange strain tensor $\boldsymbol{E}$. J is Jacobien determinant of deformation gradient tensor. Cauchy stress tensor $\boldsymbol{\sigma}$ could be expressed as the sum of two other stress tensors which are volumetric stress tensor $\boldsymbol{\sigma}_{vol}$ and stress deviator tensor $\overline{\boldsymbol{\sigma}}$ as Equation (3.4).

$$\boldsymbol{\sigma} = \boldsymbol{\sigma}_{vol} + \overline{\boldsymbol{\sigma}} \tag{3.4}$$

where $\boldsymbol{\sigma}_{vol} = p\boldsymbol{I}$ and p is Lagrange multiplier to descript the incompressibility of the artery wall (Shigley and Mischke, 2001; Fung, 1994; Fung, 1985; Fung, 1990).

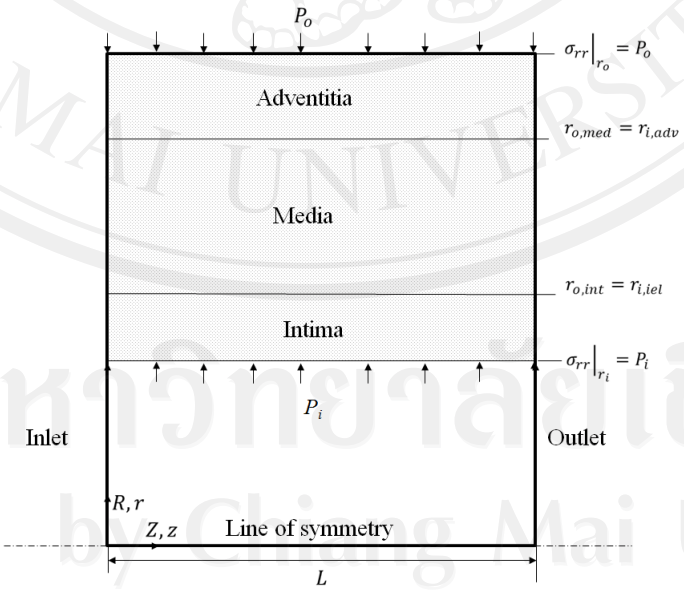

Figure 3.7 Boundary conditions

3.2.2.2. Computational model

Boundary conditions shows in Figure 3.7. Thickness ratio of media and adventitia is set as 2:1 (Holzapfel and Gasser, 2000) and thickness ratio of intima and media is set as 1:20 (Yang and Vafai, 2006).

3.2.2.3. Mechanical formulations

Kinematics of the artery in cylindrical coordinate, deformation equations (Holzapfel and Gasser, 2000; Holzapfel, 2001) are as following.

$$r = \sqrt{\frac{R^2 - R_i^2}{k\lambda_z} + r_i^2}, \tag{3.5}$$

$$\theta = k\Theta + Z\frac{\Phi}{L}, \tag{3.6}$$

$$z = \lambda_z Z \tag{3.7}$$

where $k = \frac{2\pi}{(2\pi - \alpha)}$, λ_z is stretch ratio in longitudinal direction, Φ and L are opening angle and overall length of artery in reference configuration and subscript i in Equation (3.5) refers to inside.

According to the artery structure composted of fiber and non-collagen matrix of material, fiber reinforced strain energy function suggested by G.A.Holzapfel (2000) had been suitable used to relate stress and strain. The strain energy function could be written in two terms of isotropic and anisotropic deformations as Equation (3.8).

$$\bar{\Psi}_j = \frac{c_j}{2}(\bar{I}_1 - 3) + \frac{k_{1j}}{2k_{2j}}\sum_{i=4,6}\left\{exp\left[k_{2j}\left(\bar{I}_{ij} - 1\right)^2\right] - 1\right\} \tag{3.8}$$

where $c_j > 0$, $k_{1j} > 0$ are stress-like parameter and $k_{2j} > 0$ is dimensionless parameter, subscript *j* refer to intima, media and adventitia layers (see Figure 3.7) and subscript i refer to index number of invariants. In Equation (3.8), $\bar{I}_1$ is the first principal invariant of $\overline{\boldsymbol{C}}$ and the definitions of the invariants in Equation (3.9) associate with the anisotropic deformation of arterial wall.

$$\bar{I}_{4j} = \overline{\boldsymbol{C}} : \boldsymbol{A_{1j}}, \bar{I}_{6j} = \overline{\boldsymbol{C}} : \boldsymbol{A_{2j}} \tag{3.9}$$

The collagen fiber is assumed that it do not support compressive stress. Thus, in case of $\bar{I}_{4j} \leq 1$and $\bar{I}_{6j} \leq 1$ the response is similar to the response of rubber like material that descripted by Neo-Hookean functions. The tensor $\boldsymbol{A_{1j}}$ and $\boldsymbol{A_{2j}}$ characterizing the structure are given by Equation (3.10).

$$\boldsymbol{A_{1j}} = \boldsymbol{a_{01j}} \otimes \boldsymbol{a_{01j}}, \boldsymbol{A_{2j}} = \boldsymbol{a_{02j}} \otimes \boldsymbol{a_{02j}} \tag{3.10}$$

Component of the direction vector $\boldsymbol{a_{01j}}$ and $\boldsymbol{a_{02j}}$ in cylindrical coordinate system are in forms as Equation (3.11).

$$\boldsymbol{a_{01j}} = \begin{bmatrix} 0 \\ \cos\beta_j \\ \sin\beta_j \end{bmatrix}, \ \boldsymbol{a_{02j}} = \begin{bmatrix} 0 \\ \cos\beta_j \\ -\sin\beta_j \end{bmatrix} \tag{3.11}$$

where β_j is the angle between the collagen fibers and circumferential direction.

Hence, the stress in Eulerian description could be determined by the expression in Equation (3.12).

$$\bar{\boldsymbol{\sigma}}_{\boldsymbol{j}} = c_j \, dev\bar{\boldsymbol{b}} + \sum_{i=4,6} 2\bar{\Psi}_{ij} \, dev\left(\boldsymbol{a_{ij}} \otimes \boldsymbol{a_{ij}}\right) \tag{3.12}$$

where $\bar{\Psi}_{ij} = \frac{\partial \bar{\Psi}_{aniso}}{\partial \bar{I}_{ij}}$ denotes as response function and $\boldsymbol{a_{ij}} = \bar{\boldsymbol{F}}\boldsymbol{a_{oij}}$ denotes as Eulerian counter part of $\boldsymbol{a_{oij}}$. The equilibrium equation in cylindrical coordination in equation (3.13) is used with boundary equations. Inside pressure from the model and the equations to predict stresses distributions are provided.

$$\frac{\partial \boldsymbol{\sigma}}{\partial \boldsymbol{x}} = \mathbf{0} \tag{3.13}$$

3.2.2.4. Determination constitutive parameters

There are three parameters in each arterial layers which must be estimated to apply in equations of stresses. Nonlinear lease square method is used to estimate these relevant parameters by minimizes function of mean square error (*MSE*) of pressures in form as Equation (3.14)

$$MSE_{par} = \frac{1}{N}\sum_{l=1}^{N}\left(p_{i,model} - p_{i,experiment}\right)^2 \tag{3.14}$$

where N is number of longitudinal data points.

The Pearson product moment correlation coefficient r_{par} through the data points in $p_{i,model}$ and $p_{i,experiment}$ is used for the agreement of fit. The Equation for the Pearson product moment correlation coefficient r_{par} is

$$r_{par} = \frac{\sum_{i=1}^{N}\left(p_{i,model} - \overline{p}_{i,model}\right)\left(p_{i,experiment} - \overline{p}_{i,experiment}\right)}{\sqrt{\sum_{i=1}^{N}\left(p_{i,model} - \overline{p}_{i,model}\right)^2 \sum_{i=1}^{N}\left(p_{i,experiment} - \overline{p}_{i,experiment}\right)^2}} \tag{3.15}$$

where N is number of longitudinal data points and i is index for summation over the whole data points.

3.3. Mechanical modeling of blood vessel for human aortic vessel

Cardiovascular system has a heart acted as a pump, arteries system served to convert pulsatile flow pumped by heart to steady flow in peripheral vessels and vein system acted as reservoir of returned blood before return to the heart to complete cycle of cardiovascular blood flow. To normally serve fresh blood to body, artery is important role. The pressure resulting from blood flow acts in endothelium cells of artery. The endothelium cells response to the stress and to strain by inflation or contraction and extension. To prevent unrequired failure of artery, the initiation and propagation of rupture area should be predicted and assessment of rupture area should be qualitatively observed. Mechanical properties of stress and strain of the arterial wall have received more attention in recent. Several constitutive models have been proposed (Holzapfel *et al.*, 2000; Delfino *et al.*, 1997; Fung, 1990; Fung, 1997; Fung, 1993). Monolayer homogenous arterial wall is simple way to study. However, it is

well known the arterial wall is non-homogeneous material. A better approach is to model heterogeneity of the arterial wall by considering as multi-layer according to its histology. The arterial wall is modelled as several different layers, i.e. endothelium, intima, internal elastic lamina, media and adventitia and this model couples the blood flow through lumen causing pressure acted on inside surface of arterial wall. Stress and strain are mechanical concept based on continuum model developed to interpret concentration of force and deformation of arterial wall. There are many definitions of stress and strain (Fung, 1969; Fung, 1994; Fung, 2001). In present study, the Cauchy stress and the Green-Lagrange strain are used to refer force acted on deformed area and ratio of inflation and extension. These are for simple physics quantify.

Although, biological tissue might not directly to the stress and strain in that it might be excited by various basic quantities such as chemical action which are generally difficult to measure, measured stress and strain are therefore quantitatively important. By monitoring stress and strain during a cyclic load experiment, the response of the artery could be clearly identified that the load and unloading paths show only small hysteresis (Holzapfel at al., 2004). Stress and strain behavior of arterial wall hence involve with elastic deformation under the pressure load. The main purpose of this section is to develop three-dimension five-layer model for study effect of pressure on arterial failure. In particular, levels of pressure are studied and rupture area is consequently predicted.

3.3.1. Experimental data harvest

3.3.1.1. Luminal pressure

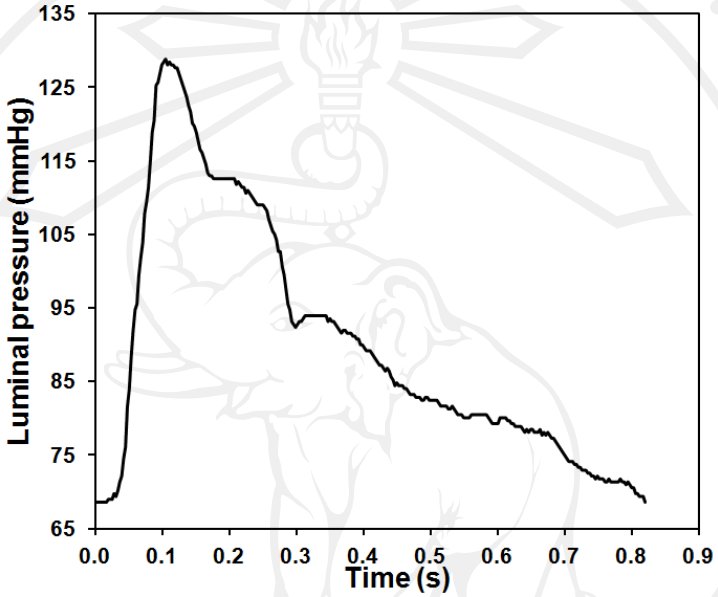

Figure 3.8 The pressure profile along a cardiac cycle at carotid artery of human (Male, Time step=0.140014 ms, N =5852 points, Cardiac cycle time=Time step*(N -1)=0.8192 s, Heart rate=73.240 bpm). Experimental data are supported by Ultrasound and Elasticity Imaging Laboratory (UEIL), Biomedical Engineering and Radiology, Columbia University, New York, USA.

Lumen region is considered to obtain luminal pressure variation acted on inside surface of artery and experimental data of pressure are required. Experimental data is examined from healthy American volunteer with age of 28 year old. The pressure profile from experimental data (N =5852) at carotid artery of human supported by UEIL (Ultrasound and Elasticity Imaging Laboratory (UEIL),

Biomedical Engineering and Radiology, Columbia University, New York, USA) are shown in Figure 3.8. Methodology to obtain the pressure (Khamdaeng *et al.*, 2011) is briefly explained as following. To obtain pressure wave form, the applanation tonometer (Millar SPT-301 probe; Millar Instruments, Houston, TX) is placed on the subject at wrist against the radial artery and the strongest pulse signal is manually detected. Since diastolic blood pressure (DBP) and systolic blood pressure (SBP) are equal to those of the brachial artery (Payne at el., 2007), the radial pressure waveform is calibrated via a SphygmoCor system (AtCor medical, Sydney, NSW, Australia) using the brachial blood pressure measured by a sphygmomanometer. To obtain magnitude of pressure waveform, a sensor is placed perpendicularly on the carotid artery and measures the mean blood pressure (MBP) and diastolic blood pressure (DBP). The pressure profile is then obtained.

3.3.1.2. Displacement

The diameter profile from experimental data (N =404) at carotid artery of human supported by UEIL (Ultrasound and Elasticity Imaging Laboratory (UEIL), Biomedical Engineering and Radiology, Columbia University, New York, USA) are shown in Figure 3.9. Methodology to obtain the diameter is briefly explained as following. The ultrasound probe is placed on the skin at the carotid position. Ultrasound gel is used as a coupling medium to acquire RF signals. High temporal resolution RF frames of the carotid are obtained by using 10-MHz linear array transducer and clinical ultrasound system (Sonix TOUCH; Ultrasonix Medical, Burnaby, British Columbia, Canada). Cross-correlation technique (Luo and Konofagou, 2010) is used to estimate the wall displacement from the ultrasound radio

frequency (RF) signals acquired at a frame rate of 505 Hz and determined between consecutive RF frames acquired at a sampling frequency of 20 MHz, depth of 30 mm, width of 38 mm, and a line density from 16 to 32 beams. Regarding cross-correlation technique, the cumulative displacement was calculated. The diameter of the carotid artery could be obtained.

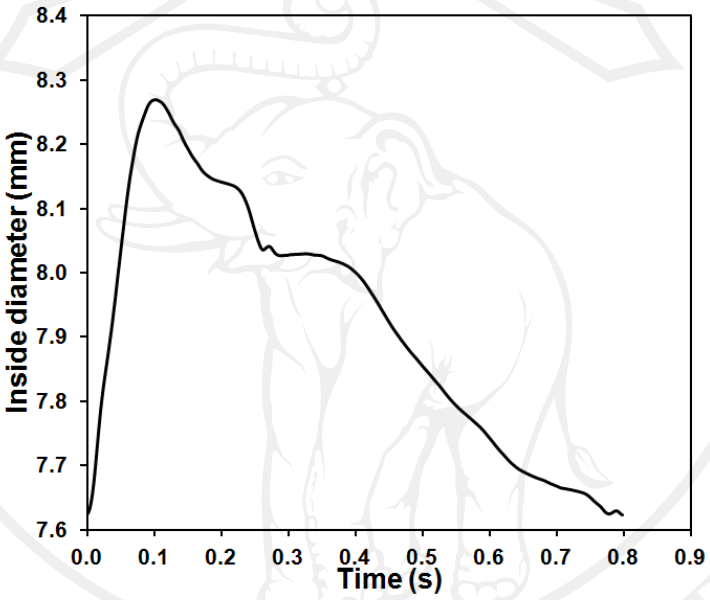

Figure 3.9. The diameter profile along a cardiac cycle at carotid artery of human (Time step= 1/505 ms, N = 404 points, Cardiac cycle time= Time step*(N -1)= 0.7980 sec, Heart rate= 75.186 bpm). Experimental data are supported by Ultrasound and Elasticity Imaging Laboratory (UEIL), Biomedical Engineering and Radiology, Columbia University, New York, USA.

3.3.2. Mechanical modeling

3.3.2.1. Continuum mechanics

Continuum mechanics Equations provide us to descript properties of stress and strain responses of the arterial wall. Continuum mechanics knowledge is excellently reviewed by Y. C. Fung (Fung, 1969; Fung, 1994). The stress is always understood to be the force acted on arterial wall per unit area and related to deformation of the arterial wall described by strain. Classical knowledge of conservation equations, strain-displacement equations and appropriated constitutive equation are applied with boundary conditions to determine these stress and strain responses that are afterward important to consider rupture of arterial wall.

The mathematical description of deformation is interested in movement of the arterial wall. Once the arterial wall is moved every particle of arterial medium is going to new position. Consider the body of arterial wall in the reference configuration Ω_o, every material particle point in cylindrical coordinate is given as $\boldsymbol{X}(R,\Theta,Z)$. By the time that the body of arterial wall is deformed, the material point $\boldsymbol{X}(R,\Theta,Z)$ transforms to position $\boldsymbol{x}(r,\theta,z)$ or its inverse in deformed configuration Ω. The features of transformation described the deformation are given by the first partial derivatives of these two configurations relationships called the deformation gradient tensor $\boldsymbol{F}$ and written as

$$\boldsymbol{F} = \frac{\partial \boldsymbol{x}}{\partial \boldsymbol{X}}. \tag{3.1}$$

The deformation gradients could be used to describe the distance between two neighboring points in these two configurations and the Green-Lagrange strain tensor $\boldsymbol{E}$ could be introduced as equation

$$\boldsymbol{E} = \frac{1}{2}(\boldsymbol{C} - \boldsymbol{I}). \tag{3.3}$$

This form of the Green-Lagrange strain tensor $\boldsymbol{E}$ is in terms of the right Cauchy Green tensor $\boldsymbol{C}$ which is

$$\boldsymbol{C} = \boldsymbol{F}^T \boldsymbol{F} \tag{3.2}$$

and $\boldsymbol{I}$ denotes identity tensor.

The internal force reacted to external force and acting within deformed body per unit area could be measured as stress. To describe the hyperelastic stress response of arterial wall, appropriate strain energy function Ψ is chosen to describe physical behavior of arterial wall. The force in the reference configuration Ω_o to area in the reference configuration Ω_o well-known as the second Piola–Kirchhoff stress tensor $\boldsymbol{S}$ could be determined by performing the first derivative of strain energy function Ψ respected to the Green-Lagrange strain tensor $\boldsymbol{E}$ as

$$\boldsymbol{S} = \frac{\partial \Psi}{\partial \boldsymbol{E}}. \tag{3.16}$$

The Piola–Kirchhoff stress tensor could be transformed to the Cauchy stress tensor via relationship of

$$\boldsymbol{\sigma} = J^{-1}\boldsymbol{F}\boldsymbol{S}\boldsymbol{F}^{T} \tag{3.17}$$

where J denotes Jacobian determinant of deformation gradient tensor which must satisfy the condition of conservation of mass whose value is greater than zero.

The Cauchy stress tensor $\boldsymbol{\sigma}$ could be expressed as the sum of two other stress tensors which are volumetric stress tensor $\boldsymbol{\sigma}_{vol}$ which tends to change the volume of the stressed body and stress deviator tensor $\overline{\boldsymbol{\sigma}}$ which tends to distort the stressed body that is

$$\boldsymbol{\sigma} = \boldsymbol{\sigma}_{vol} + \overline{\boldsymbol{\sigma}}. \tag{3.4}$$

The equation of motion of a continuum derived by applying Newton's law is in form

$$\frac{\partial \boldsymbol{\sigma}}{\partial \boldsymbol{x}} + \boldsymbol{G} = \rho \boldsymbol{a} \tag{3.18}$$

where $\boldsymbol{G}$ denotes body force of arterial wall and $\boldsymbol{a}$ denoted its acceleration.

The conservation of mass is expressed by

$$\frac{\partial \rho}{\partial t} + \frac{\partial \rho \boldsymbol{v}}{\partial \boldsymbol{x}} = \boldsymbol{0} \tag{3.19}$$

where this ρ denotes density of arterial wall and $\boldsymbol{v}$ denotes its velocity vector.

The deformation of the arterial wall is related to the luminal pressure as applied load by blood flow in arterial lumen. The blood considered as an incompressible Newtonian fluid could be descripted by the Navier-Stokes equation as

$$\rho \frac{\partial \boldsymbol{v}}{\partial t} + \rho \boldsymbol{v}.\nabla \boldsymbol{v} = -\nabla p + \mu \nabla^2 \boldsymbol{v} + \boldsymbol{f} \tag{3.20}$$

where this ρ denotes density of blood, $\boldsymbol{v}$ denotes velocity vector, p denoted luminal pressure, μ denotes dynamic viscosity of blood and $\boldsymbol{f}$ denotes its body force.

Hence, the stress and strain distributions in arterial wall could be predicted and then used for rupture consideration.

3.3.2.2. Computational model

A three-dimension five-layer mechanical model is developed for prediction of stresses and strains distributions across arterial wall in a cardiac cycle. The schematic illustration of idealized artery geometry and boundary conditions under consideration is shown in Figure 3.10.

a) Geometry of arterial wall

The arterial geometry is idealized as a five concentric axisymmetric layers straight circular cylindrical nonlinear elastic tube. In reference configuration luminal radius R of 3.1 mm, longitudinal length L of 124 mm (Yang

and Vafai, 2006) and thickness of each arterial wall layer is presented in Table 1 and the adventitia is assumed that occupies a half of the media.

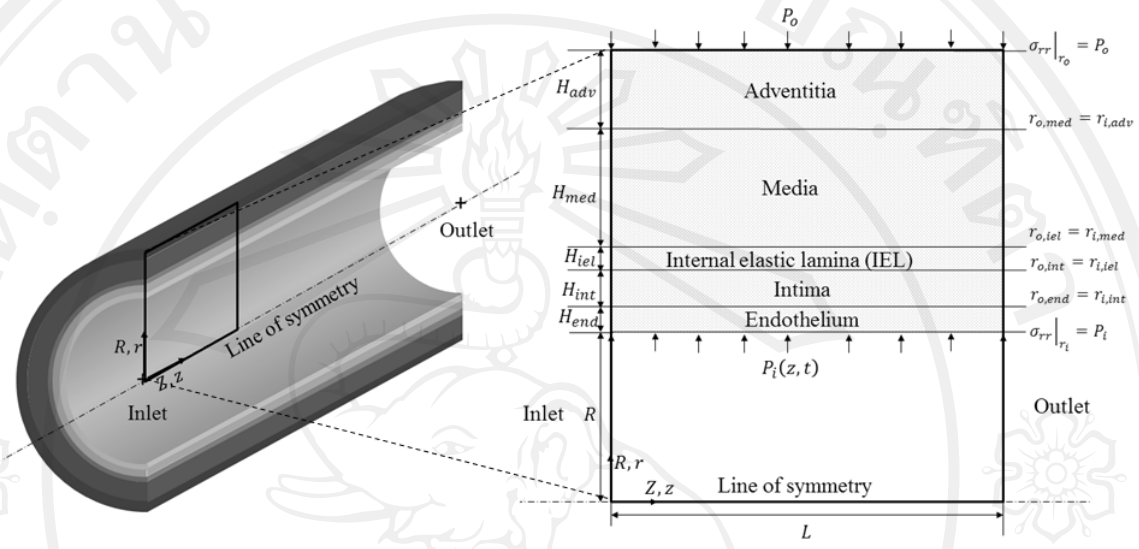

Figure 3.10 Schematic illustration of the geometric artery and boundary conditions

Table 3.1 Thickness of each wall layer of artery (Yang and Vafai, 2006; Ai and Vafai, 2006; Yang and Vafai, 2008)

Wall layer	Symbol	Thickness (μ m)
Endothelium	H_{end}	2.0
Intima	H_{int}	10.0
Internal elastic lamina (IEL)	H_{iel}	2.0
Media	H_{med}	200.0
Adventitia	H_{adv}	100.0

b) Boundary conditions

Since blood flows in the lumen of arterial as pulse, the blood pressure acted to inside arterial wall surface causes the wall movement which is assumed that the pressure is uniform in circumferential direction and perpendicular to arterial wall surface at certain longitudinal position. Pressure acted to outside arterial

wall surface is assumed as uniform pressure with magnitude of 30 mmHg. The geometries of the five layers are compatible which means that outside radius of the individual wall layer is the same as inside radius of its outward neighbour layer.

3.3.2.3. Mechanical formulations

There are six regions in present mechanical model, i.e. lumen and five arterial layers of endothelium, intima, internal elastic lamina, media and adventitia. As starting from continuum mechanics, the mathematical formulations for each region are following.

a) Lumen

Lumen region is considered to obtain luminal pressure variation acted on inside surface of artery and experimental data of pressure are required. The pressure profile from experimental data (N =5852) at carotid artery of human supported by UEIL (Ultrasound and Elasticity Imaging Laboratory (UEIL), Biomedical Engineering and Radiology, Columbia University, NY, US) are shown in Figure 3.11. Blood flows through arterial lumen which the blood is considered as an incompressible Newtonian fluid could be descripted by the Navier-Stokes equation of Equation (3.20). The Navier-Stokes equation expressed in cylindrical coordinates could be expanded as

$$\rho\left(\frac{\partial u_r}{\partial t}+u_r\frac{\partial u_r}{\partial r}+\frac{u_\theta}{r}\frac{\partial u_r}{\partial \theta}+u_z\frac{\partial u_r}{\partial z}-\frac{u_\theta^2}{r}\right)=-\frac{\partial p}{\partial r}+\mu\left[\frac{1}{r}\frac{\partial}{\partial r}\left(r\frac{\partial u_r}{\partial r}\right)+\frac{1}{r^2}\frac{\partial^2 u_r}{\partial \theta^2}+\frac{\partial^2 u_r}{\partial z^2}-\frac{u_r}{r^2}-\frac{2}{r^2}\frac{\partial u_\theta}{\partial \theta}\right]+\rho f_r \tag{3.21}$$

$$\rho\left(\frac{\partial u_\theta}{\partial t}+u_r\frac{\partial u_\theta}{\partial r}+\frac{u_\theta}{r}\frac{\partial u_\theta}{\partial \theta}+u_z\frac{\partial u_\theta}{\partial z}+\frac{u_r u_\theta}{r}\right)=-\frac{1}{r}\frac{\partial p}{\partial \theta}+\mu\left[\frac{1}{r}\frac{\partial}{\partial r}\left(r\frac{\partial u_\theta}{\partial r}\right)+\frac{1}{r^2}\frac{\partial^2 u_\theta}{\partial \theta^2}+\frac{\partial^2 u_\theta}{\partial z^2}+\frac{2}{r^2}\frac{\partial u_r}{\partial \theta}-\frac{u_\theta}{r^2}\right]+\rho f_\theta \tag{3.22}$$

$$\rho\left(\frac{\partial u_z}{\partial t}+u_r\frac{\partial u_z}{\partial r}+\frac{u_\theta}{r}\frac{\partial u_z}{\partial \theta}+u_z\frac{\partial u_z}{\partial z}\right)=-\frac{\partial p}{\partial z}+\mu\left[\frac{1}{r}\frac{\partial}{\partial r}\left(r\frac{\partial u_z}{\partial r}\right)+\frac{1}{r^2}\frac{\partial^2 u_z}{\partial \theta^2}+\frac{\partial^2 u_z}{\partial z^2}\right]+\rho f_z \tag{3.23}$$

where $\boldsymbol{v}=\left[u_r(r,\theta,z)\quad u_\theta(r,\theta,z)\quad u_z(r,\theta,z)\right]$, u_r, u_θ and u_z are components of velocity vector, f_r, f_θ and f_z are components of body force by subscript r, θ and z refer to radial, circumferential and longitudinal directions, respectively.

Blood flow is pulsatile and characterized by a fully develop or parabolic velocity profile at the inlet of the arterial lumen. The velocity profile is assumed to be axisymmetric as

$$u_z=U_{cl}\left(1-\left(\frac{r}{R}\right)^2\right) \tag{3.24}$$

where U_{cl} is the centerline velocity at the lumen inlet.

The lumen is horizontal so that the gravity effect could be ignored and axisymmetric flow is assumed thus no tangential and radial velocities and the remaining quantities are independent of θ. The Navier-Stokes expanding equations could be reduced to be as

$$\frac{\partial p}{\partial r}=0,\ \frac{\partial p}{\partial \theta}=0,\ \rho\frac{\partial u_z}{\partial t}+u_z\frac{\partial u_z}{\partial z}=-\frac{\partial p}{\partial z}+\mu\frac{\partial^2 u_z}{\partial r^2}+\mu\frac{\partial^2 u_z}{\partial z^2}. \tag{3.25}$$

The centerline velocity at the lumen inlet is specified by a simple time-dependent sinusoidal function as

$$U_{cl} = U_o\left(1+\delta\sin\left(\frac{2\pi t}{T}\right)\right) \tag{3.26}$$

and then used to characterize pulsatile flow in the artery where T is the period of the pulsatile blood flow, δ is the parameter used to account for the fluctuation of the pulsatile flow during each cardiac cycle and U_o is reference bulk inflow velocity.

Substituting equation of U_{cl} as Equation (3.26) into equation of u_z as Equation (3.24) and then into reducing equation of Navier-Stokes in longitudinal direction as the third one of Equation (3.25), it could be obtained equation as

$$\rho U_o\left(1-\left(\frac{r}{R}\right)^2\right)\delta\left(\frac{2\pi}{T}\right)\cos\left(\frac{2\pi t}{T}\right) = -\frac{\partial p}{\partial z} - \frac{2\mu U_o}{R^2}\left(1+\delta\sin\left(\frac{2\pi t}{T}\right)\right). \tag{3.27}$$

Pressure gradient at inside arterial wall could be easily determined by using $r = R$, we have

$$\frac{\partial p}{\partial z} = -\frac{2\mu U_o}{R^2}\left(1+\delta\sin\left(\frac{2\pi t}{T}\right)\right). \tag{3.28}$$

Negative sign presents to pressure drop in lumen due to viscosity of blood. Pressure along a cardiac cycle and pressure variation with longitudinal direction $p(z,t)$ could be consequently expressed as

$$p(z,t)=\left(\frac{2\mu U_o}{R^2}\left(1+\delta\sin\left(\frac{2\pi t}{T}\right)\right)\right)(z_{outlet}-z)+p_{outlet}(t). \quad (3.29)$$

Since $p_{outlet}(t)$ is time dependent. Equation of this pressure profile along a cardiac cycle could be obtained by curve fitting using Fourier approximation with mean squares error fit of a sinusoid with the experimental data of pressure. The equation form of this pressure profile (Chapra and Canale, 2010) is

$$p_{outlet}(t)=\mathbb{A}_0+\mathbb{A}_1\cos\left(\frac{2\pi t}{T}\right)+\mathbb{B}_1\sin\left(\frac{2\pi t}{T}\right)+\mathbb{A}_2\cos\left(2*\frac{2\pi t}{T}\right)$$
$$+\mathbb{B}_2\sin\left(2*\frac{2\pi t}{T}\right)+\cdots+\mathbb{A}_j\cos\left(j*\frac{2\pi t}{T}\right)+\mathbb{B}_j\sin\left(j*\frac{2\pi t}{T}\right) \quad (3.30)$$

where the coefficients while equally time step could be evaluated by

$$\mathbb{A}_0=\frac{\sum_{i=1}^{N}p_i}{N},\ \mathbb{A}_j=\frac{2}{N}\sum_{i=1}^{N}p_i\cos\left(j*\frac{2\pi t}{T}\right),\ \mathbb{B}_j=\frac{2}{N}\sum_{i=1}^{N}p_i\sin\left(j*\frac{2\pi t}{T}\right) \quad (3.31)$$

and $I=1,2,\ldots,N$, $J=1,2,\ldots,k$, N is number of data points and k is number of sinusoidal finite series.

Mean square error MSE_p used to quantify the different between obtained outlet pressure equation and experimental pressure data could be determined by

$$MSE_p = \frac{1}{N}\sum_{i=1}^{N}\left\{p_i - \left[\mathbb{A}_0 + \sum_{j=1}^{k}\mathbb{A}_j\cos\left(j * \frac{2\pi t}{T}\right) + \mathbb{B}_j\sin\left(j * \frac{2\pi t}{T}\right)\right]\right\}^2. \quad (3.32)$$

It should be noted that in the event of number of sinusoidal finite series k is equal to number of data points N, it is approach to the continuous Fourier series.

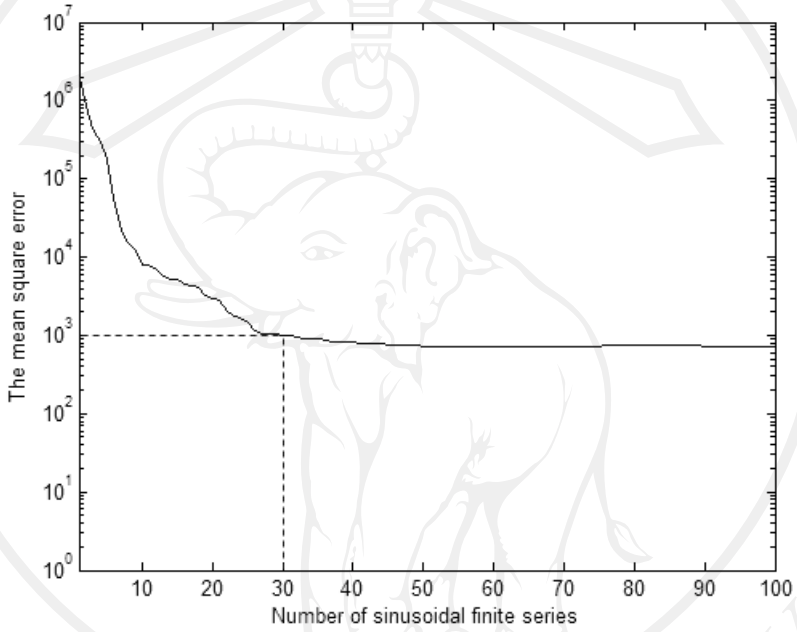

Figure 3.11 Mean square error MSE_p and number of sinusoidal finite series k relationship plotted in semi-log scale

Because there is a large number of data point, it results to large number of terms in outlet pressure equation. Hence, the pressure profile is attempted to be fit with k only in range of 1 to 100 by additional reason of computational time as well. In order to find suitable number of sinusoidal finite series k, mean square error MSE_p and number of sinusoidal finite series k relationship should be plotted in semi-log scale as Figure 3.11. It is clear that it is not necessary to use number of sinusoidal finite series k equal to number of data points N because nearly constant in order of

magnitude of MSE_p is obtained in range of number of sinusoidal finite series about 30 to 100. Thus, suitable number of sinusoidal finite series k could be obtained as 30. Therefore, the equation of the pressure profile could be expressed by using suitable number of sinusoidal finite series k as

$$p_{outlet}(t) = \mathbb{A}_0 + \sum_{j=1}^{30} \mathbb{A}_j \cos\left(j * \frac{2\pi t}{T}\right) + \mathbb{B}_j \sin\left(j * \frac{2\pi t}{T}\right). \quad (3.33)$$

There are three parameters served to characterize the equation of this pressure profile; the mean value $\mathbb{A}_0$ sets the average height above the abscissa, the amplitudes $\mathbb{A}_j$ and $\mathbb{B}_j$ specifies the height of the oscillation and the angular frequency $\frac{2\pi}{T}$ characterizes how often the cycles occur. Two additional parameters ζ and ξ is thus used in the equation of the pressure profile to quantify fold values of mean, $((3MBP) + SBP)/4$, and amplitude, $(3/4)(SBP - MBP)$, respected to this experimental data where MBP is mean blood pressure and SBP is systolic blood pressure. The equation could be written as

$$p_{outlet}(t) = (\zeta * \mathbb{A}_0) + \xi \sum_{j=1}^{30} \mathbb{A}_j \cos\left(j * \frac{2\pi t}{T}\right) + \mathbb{B}_j \sin\left(j * \frac{2\pi t}{T}\right). \quad (3.34)$$

Finally, pressure along a cardiac cycle and pressure variation with longitudinal direction, $p(z,t)$, could be expressed as

$$p(z,t) = \left(\frac{2\mu U_0}{R^2}\left(1 + \delta\sin\left(\frac{2\pi t}{T}\right)\right)\right)(z_{outlet} - z) + (\zeta * \mathbb{A}_0) + \xi\sum_{j=1}^{30}\mathbb{A}_j\cos\left(j * \frac{2\pi t}{T}\right) + \mathbb{B}_j\sin\left(j * \frac{2\pi t}{T}\right). \quad (3.35)$$

$p(z,t)$ is then used in this study by using blood viscosity μ of 0.0037 $\frac{\text{g}}{\text{mm.s}}$, reference bulk inflow velocity U_o of 169 $\frac{\text{mm}}{\text{s}}$, fluctuation of pulsatile flow parameter δ of 1, period of a cardiac time T of 0.8 s, parameters ζ and ξ are equal to unity, parameter $\mathbb{A}_0$ of 12011.1954 Pa, $\mathbb{A}_j$ and $\mathbb{B}_j$ as in Table 3.2.

Table 3.2 Parameters $\mathbb{A}_j$ and $\mathbb{B}_j$ in unit of Pascal

$\mathbb{A}_j$						$\mathbb{B}_j$					
$\mathbb{A}_1$	-307.802	$\mathbb{A}_{11}$	-8.0677	$\mathbb{A}_{21}$	-14.8198	$\mathbb{B}_1$	2472.354	$\mathbb{B}_{11}$	6.7722	$\mathbb{B}_{21}$	-0.7861
$\mathbb{A}_2$	-1152.17	$\mathbb{A}_{12}$	44.5415	$\mathbb{A}_{22}$	-35.7354	$\mathbb{B}_2$	899.1454	$\mathbb{B}_{12}$	-21.8575	$\mathbb{B}_{22}$	4.3848
$\mathbb{A}_3$	-904.308	$\mathbb{A}_{13}$	22.2471	$\mathbb{A}_{23}$	-5.9142	$\mathbb{B}_3$	141.6018	$\mathbb{B}_{13}$	40.6469	$\mathbb{B}_{23}$	-19.529
$\mathbb{A}_4$	-472.175	$\mathbb{A}_{14}$	-30.1193	$\mathbb{A}_{24}$	4.3074	$\mathbb{B}_4$	-162.328	$\mathbb{B}_{14}$	-5.9916	$\mathbb{B}_{24}$	-17.2017
$\mathbb{A}_5$	-376.189	$\mathbb{A}_{15}$	18.2471	$\mathbb{A}_{25}$	-1.4468	$\mathbb{B}_5$	-319.284	$\mathbb{B}_{15}$	-3.3656	$\mathbb{B}_{25}$	-20.3007
$\mathbb{A}_6$	-12.2606	$\mathbb{A}_{16}$	21.6265	$\mathbb{A}_{26}$	22.4666	$\mathbb{B}_6$	-490.187	$\mathbb{B}_{16}$	33.2005	$\mathbb{B}_{26}$	-15.6279
$\mathbb{A}_7$	196.7156	$\mathbb{A}_{17}$	9.0006	$\mathbb{A}_{27}$	14.0872	$\mathbb{B}_7$	-193.917	$\mathbb{B}_{17}$	11.1883	$\mathbb{B}_{27}$	6.0502
$\mathbb{A}_8$	93.4258	$\mathbb{A}_{18}$	7.895	$\mathbb{A}_{28}$	8.5244	$\mathbb{B}_8$	-52.9216	$\mathbb{B}_{18}$	21.7935	$\mathbb{B}_{28}$	-2.0939
$\mathbb{A}_9$	76.1842	$\mathbb{A}_{19}$	-14.0034	$\mathbb{A}_{29}$	8.0986	$\mathbb{B}_9$	-44.6953	$\mathbb{B}_{19}$	37.0081	$\mathbb{B}_{29}$	-0.6531
$\mathbb{A}_{10}$	70.6487	$\mathbb{A}_{20}$	-20.9844	$\mathbb{A}_{30}$	6.8244	$\mathbb{B}_{10}$	58.292	$\mathbb{B}_{20}$	7.7842	$\mathbb{B}_{30}$	9.3357

b) Arterial layers

Geometry and boundary conditions show in Figure 3.10 is in reference configuration. Continuum mechanics applied to biological tissue could systemically understand by reviewing in literatures of Fung and Humphrey (Fung, 1990; Fung, 1997; Fung, 1993; Fung, 2001; Humphrey, 2002). Kinematics of the

artery in cylindrical coordinate, deformation equations (Holzapfel *et al.*, 2000) are as following.

$$r = \sqrt{\frac{R^2 - R_i^2}{k\lambda_z} + r_i^2}\,, \tag{3.5}$$

$$\theta = k\Theta + Z\frac{\Phi}{L}\,, \tag{3.6}$$

$$z = \lambda_z Z \tag{3.7}$$

where $k = \dfrac{2\pi}{2\pi - \alpha}$, λ_z is stretch ratio in longitudinal direction which the value of 1.1 is applied (Delfino *et al.*, 1997) for every layer, Φ and L are opening angle and overall length of artery in reference configuration and subscript i in Equation (3.5) refers to inside. The artery deformed under extension and inflation and without residual strain is considered in this study.

For endothelium and internal elastic lamina, the strain energy function of neo-Hookean has been used to determine nonlinear response. The strain energy function for incompressible neo-Hookean material is

$$\overline{\Psi}_j = \frac{c_j}{2}\left(\bar{I}_1 - 3\right) \tag{3.36}$$

where $c_j > 0$ is stress-like parameter, $\bar{I}_1$ is the first principal invariant of $\overline{\boldsymbol{C}}$ and subscript j refer to endothelium and internal elastic lamina (IEL). There is only one parameter of c for each layer.

For intima, media and adventitia, according to the artery structure composted of fibers and non-collagen matrix of material, fiber reinforced strain energy function suggested by Holzapfel *et al.* (2000) has been suitable used to relate stress and strain. The major reason that this fiber reinforced strain energy function is suitable used is not only it takes account of architecture of the arterial wall but also it is relevant relatively small number of parameters (Khakpour and Vafai, 2008; Holzapfel *et al.*, 2004; Holzapfel *et al.*, 2005). The strain energy function could be written in two terms of isotropic and anisotropic as Equation (3.8).

$$\overline{\Psi}_j = \frac{c_j}{2}\left(\bar{I}_1 - 3\right) + \frac{k_{1j}}{2k_{2j}} \sum_{i=4,6} \left\{ \exp\left[k_{2j}\left(\bar{I}_{ij} - 1\right)^2 \right] - 1 \right\} \tag{3.8}$$

where $c_j > 0$, $k_{1j} > 0$ are stress-like parameter and $k_{2j} > 0$ is dimensionless parameter, subscript j refer to intima, media and adventitia layers and subscript i refer to index number of invariants. In Equation (3.8), $\bar{I}_1$ is the first principal invariant of $\overline{\boldsymbol{C}}$ and the definitions of the invariants in Equation (3.9) associate with the anisotropic deformation of arterial wall.

$$\bar{I}_{4j} = \overline{\boldsymbol{C}} : \boldsymbol{A}_{1j}, \; \bar{I}_{6j} = \overline{\boldsymbol{C}} : \boldsymbol{A}_{2j} \tag{3.9}$$

The collagen fibers are assumed that it do not support compressive stress. Thus, in case of $\bar{I}_4 \le 1$ and $\bar{I}_6 \le 1$ the response is similar to the response of rubber like material

that descripted by Neo-Hookean functions. The tensor $\boldsymbol{A}_{1j}$ and $\boldsymbol{A}_{2j}$ characterizing the structure are given by Equation (3.10).

$$\boldsymbol{A}_{1j} = \boldsymbol{a}_{o1j} \otimes \boldsymbol{a}_{o1j},\ \boldsymbol{A}_{2j} = \boldsymbol{a}_{o2j} \otimes \boldsymbol{a}_{o2j} \tag{3.10}$$

Component of the direction vector $\boldsymbol{a}_{o1j}$ and $\boldsymbol{a}_{o2j}$ in cylindrical coordinate system are in forms as Equation (3.11).

$$\boldsymbol{a}_{o1j} = \begin{bmatrix} 0 \\ \cos\beta_j \\ \sin\beta_j \end{bmatrix},\ \boldsymbol{a}_{o2j} = \begin{bmatrix} 0 \\ \cos\beta_j \\ \text{-}\sin\beta_j \end{bmatrix} \tag{3.11}$$

where β_j is the angle between the collagen fibers and circumferential direction. Three different values of 5, 7 and 49 degree (Holzapfel *et al.*, 2002) are applied for the three major layers of intima, media and adventitia, respectively.

Hence, the stress in Eulerian description could be determined by the expression in Equation (3.12).

$$\bar{\boldsymbol{\sigma}}_j = c_j \mathrm{dev}\bar{\boldsymbol{b}} + \sum_{i=4,6} 2\bar{\Psi}_{ij} \mathrm{dev}\left(\boldsymbol{a}_{ij} \otimes \boldsymbol{a}_{ij}\right) \tag{3.12}$$

where $\mathrm{dev}\bar{\boldsymbol{b}} = \bar{\boldsymbol{b}} - \frac{1}{3}\left[\bar{\boldsymbol{b}} : \boldsymbol{I}\right]\boldsymbol{I}$, $\mathrm{dev}\left(\boldsymbol{a}_{ij} \otimes \boldsymbol{a}_{ij}\right) = \left(\boldsymbol{a}_{ij} \otimes \boldsymbol{a}_{ij}\right) - \frac{1}{3}\left[\left(\boldsymbol{a}_{ij} \otimes \boldsymbol{a}_{ij}\right) : \boldsymbol{I}\right]\boldsymbol{I}$,

$\boldsymbol{a}_{ij} = \bar{\boldsymbol{F}}\boldsymbol{a}_{oij}$ denotes as Eulerian counter part of $\boldsymbol{a}_{oij}$ and $\bar{\Psi}_{ij} = \frac{\partial \bar{\Psi}_{aniso}}{\partial \bar{I}_{ij}}$ denotes as

response function i.e. $\bar{\Psi}_{4j} = k_1(\bar{I}_{4j} - 1)\left(\exp\left(k_2(\bar{I}_{4j} - 1)^2\right)\right)$ and $\bar{\Psi}_{6j} = k_1(\bar{I}_{6j} - 1)\left(\exp\left(k_2(\bar{I}_{6j} - 1)^2\right)\right)$. Additionally, it should be noted that $\boldsymbol{F} = \left(J^{1/3}\boldsymbol{I}\right)\overline{\boldsymbol{F}}$, $\overline{\boldsymbol{C}} = \overline{\boldsymbol{F}}^T\boldsymbol{F}$ and $\bar{\boldsymbol{b}} = \overline{\boldsymbol{F}}\overline{\boldsymbol{F}}^T$. While incompressibility of arterial wall is applied, $\boldsymbol{F} = \overline{\boldsymbol{F}}$, $\boldsymbol{C} = \overline{\boldsymbol{C}}$ and $\boldsymbol{b} = \bar{\boldsymbol{b}}$ are obtained. There are only three parameters of c, k_1 and k_2 for each layer.

3.3.2.4. Determination constitutive parameters

In order to estimate involving parameters, luminal pressure and diameter of artery are required. Methodology to obtain the pressure of artery had already explained. The diameter profile from experimental data (N =404) at carotid artery of human supported by UEIL (Ultrasound and Elasticity Imaging Laboratory (UEIL), Biomedical Engineering and Radiology, Columbia University, NY, US) are shown in Figure 3.9. The minima and maxima of the pressure and diameter waveforms are aligned and matched over a cardiac cycle. The viscosity effect is hence ignored. Arterial wall is considered as an incompressible material and in horizontal so the gravity effect could be ignored. The equilibrium equation in Equation (3.13) is used with boundary conditions.

$$\frac{\partial \boldsymbol{\sigma}}{\partial \boldsymbol{x}} = \mathbf{0} \tag{3.13}$$

Luminal pressure could be determined by

$$p_i = \int_{r_i}^{r_o} \left(\bar{\sigma}_{\theta\theta} - \bar{\sigma}_{rr} \right) \frac{dr}{r} + p_o \tag{3.37}$$

where $\sigma_{\theta\theta} = P + \bar{\sigma}_{\theta\theta}$, $\sigma_{rr} = P + \bar{\sigma}_{rr}$ and P is Lagrange multiplier used to enforce incompressibility constrain.

There are only one parameter for each layer of endothelium and internal elastic lamina (IEL) and only three parameters for each layer of intima, media and adventitia. Although continuum mechanics provides non complicate equations, mathematics approach to the solution is quit complexity. It is different from engineering material acted as rigid body while it is subjected by pressure load. Biological tissue is moved with the pressure load changed by time. Moving boundary has faced for solving the solution in the five-layer model. Normalizing the moving boundary is employed. Numerical integration of three-point Gaussian quadrature which has accuracy order of five is employed to discrete Equation (3.37) and used with the boundary conditions. Nonlinear least square method is used to estimate these relevant parameters by minimize function of mean square error MSE_{par} of luminal pressures called 'Objective function' in form as Equation (3.14).

$$MSE_{par} = \frac{1}{N} \sum_{i=1}^{N} \left(p_{i,model} - p_{i,experiment} \right)^2 \tag{3.14}$$

The Equation for the Pearson product moment correlation coefficient r_{par} is

$$r_{par} = \frac{\sum_{i=1}^{N} \left(p_{i,model} - \bar{p}_{i,model} \right) \left(p_{i,experiment} - \bar{p}_{i,experiment} \right)}{\sqrt{\sum_{i=1}^{N} \left(p_{i,model} - \bar{p}_{i,model} \right)^2 \sum_{i=1}^{N} \left(p_{i,experiment} - \bar{p}_{i,experiment} \right)^2}} \tag{3.15}$$

where N is number of longitudinal data points and i is index for summation over the whole data points.

3.3.2.5. Arterial rupture

The artery is subjected by luminal pressure which acts on the inside surface of arterial wall resulting to the arterial wall movement. The luminal pressure and the wall movement are involved with the stress and the strain of arterial wall. If the pressure is high and the artery has inappropriate deformation, the rupture of arterial wall would occur. There are a number of researchers who study ultimate tensile stress and associated stretch in normal human artery (Holzapfel, 2001; Zohdi *et al.*, 2004; Franceschini *et al.*, 2006; Sommer *et al.*, 2008; Mohan and Melvin, 1982; Mohan and Melvin, 1983). In recent decade ultimate values of separated layers has been studied (Sommer *et al.*, 2008; Holzapfel *et al.*, 2005; Holzapfel, 2009; Zhao *et al.*, 2008; Sommer, 2010; Holzapfel *et al.*, 2004). The ultimate tensile stress and associated ultimate stretch (Holzapfel *et al.*, 2004) shown in Table 3.3 in circumferential and longitudinal directions of intima, media and adventitia are used as criterions for rupture of arterial wall in present study.

Table 3.3 The ultimate tensile stress and associated ultimate stretch

Layer	Direction	Ultimate tensile stress		Ultimate stretch
Adventitia	Circumferential direction	1031.6	kPa	1.44
	Longitudinal direction	951.8	kPa	1.353
Media	Circumferential direction	202	kPa	1.27
	Longitudinal direction	188.8	kPa	1.536
Intima	Circumferential direction	488.6	kPa	1.331
	Longitudinal direction	943.7	kPa	1.255

The equivalent tensile stress σ_v and strain E_v could be computed from the Cauchy stress tensor and the Green-Lagrange strain tensor as

$$\sigma_v = \sqrt{\frac{3}{2}\left(\boldsymbol{\sigma}:\boldsymbol{\sigma} - \frac{\left(\mathrm{tr}\boldsymbol{\sigma}\right)^2}{3}\right)}, \tag{3.38}$$

$$E_v = \sqrt{\frac{3}{2}\left(\boldsymbol{E}:\boldsymbol{E} - \frac{\left(\mathrm{tr}\boldsymbol{E}\right)^2}{3}\right)}. \tag{3.39}$$

The ultimate tensile stress and associated ultimate stretch in Table 3.3 are determined for critical equivalent tensile stress $\sigma_{vj,cri}$ and strain $E_{vj,cri}$. In this study, the local failure is defined global failure or rupture since it is the beginning of completed failure. It is difficult to separate responses of arterial wall resulting from stress and strain since both of stress and stain are significant in showing the characteristics of the material of the vessel. Hence, it is difficult to change one thing without affecting another. Strategy to identify rupture area of arterial wall is that area of arterial wall

where local equivalent tensile stress and associated local equivalent strain exceed the critical values is defined to be rupture area and if it is not, it is defined to be no rupture area. Estimation of rupture risk has been referred to the local equivalent stress and strain approach. The percentage of rupture risk of arterial wall P_{risk} is defined as

$$P_{risk} = 100\sigma_j^* E_j^* \tag{3.40}$$

where σ_j^* and E_j^* are normalized values which have consistent to

$$\sigma_j^* \left\{ \sigma_j^* \middle| \text{if } \frac{\sigma_v}{\sigma_{vj,cri}} < 1, \sigma_j^* = \frac{\sigma_v}{\sigma_{vj,cri}}; \text{if } \frac{\sigma_v}{\sigma_{vj,cri}} \geq 1, \sigma_j^* = 1 \right\}, \tag{3.41}$$

$$E_j^* \left\{ E_j^* \middle| \text{if } \frac{E_v}{E_{vj,cri}} < 1, E_j^* = \frac{E_v}{E_{vj,cri}}; \text{if } \frac{E_v}{E_{vj,cri}} \geq 1, E_j^* = 1 \right\}. \tag{3.42}$$

It still lacks data for endothelium and internal elastic lamina (IEL), critical values of intima are applied in these two layers.

Results from these methodologies are shown and discussed in next chapter.